Section A-Research paper

EFFECTS OF TEMPERATURES AND STIRRING SPEEDS ON HYDROXYAPATITE POWDER ELECTROPORETIC DEPOSITION COATING OF AISI 316 L

R. B. Taqriban[1,2], D. F. Fitriyana[2,3], Y. M Pusparikita[4], R.Ismail[1,2], J. Jamari[1], A P Bayuseno[1,*]

[1]Department of Mechanical Engineering, Diponegoro University, Semarang, Central Java, Indonesia
[2]Center for Bio Mechanics Bio Material Bio Mechatronics and Bio Signal Processing (CBIOM3S), Semarang, Central Java, Indonesiarilo. *Corresponding author: apbayuseno@gmail.com
[3]Department of Mechanical Engineering, UniversitasNegeri, Semarang, Central Java Indonesia
[4]Department of Environmental Engineering, Diponegoro University, Semarang, Central Java Indonesia

ABSTRACT

Hydroxyapatite (HA) powder is now available as a bioceramic precursor for numerous biomedical implants. Since it has excellent bioactivity, biocompatibility, and osteointegration properties, it can be formed in bulk or as a coating on metallic substrates. The current study focused on controlling temperature and stirring rates utilizing electrophoretic deposition (EPD) in nitric acid colloidal solutions for coating HA powder on stainless steel (SS316L). A fixed set of operating parameters, such as colloidal solution concentrations and compositions, electric fields, and deposition times, were used in this EPD experiment. XRD qualitative examination revealed the formation of αtricalcium phosphate (α-TCP) from hydroxyapatite decomposition on the surface coating. The operating settings have a considerable impact on the yields of deposition materials. This α-TCP layer coating is the potential to improve biocompatibility as a biomedical implant.

Keyword: Coating;Temperature; Electrophoretic deposition: Hydroxyapatite;Stirring speed

1. INTRODUCTION

Stainless steel (SS) alloys are non-toxic metallic materials with good biological safety features, appropriate for orthopedic applications and dental implants (Samani et al., 2023).

Because of its superior corrosion resistance, stainless steel AISI 316L is ideal for artificial joints, spinal fixation fixtures, orthopaedic screws, and wires. (Kravanja and Finšgar, 2022; Pani et al., 2022). However, SS alloys have weak chemical interactions with natural bones for medical implants, necessitating a biocompatible bioceramic coating to achieve osseointegration. In this case, hydroxyapatite (HA) is proposed as a bioactive ceramic for surface coating of implants because it has a similar inorganic component of the bone with strong biocompatibility and bioactivity that can respond to body temperature and physiological pH. However, HA particles may not hinder bone growth present in coating implants. Instead, significant surface cracks of implants may impair their corrosion resistance, leading to low mechanical strength and limiting their use in treatment and load-bearing applications (Gao et al. 2015).

As a result, adding carboxymethyl, cellulose, and chitosan to HA coatings may increase mechanical properties (Gebhardt et al., 2012; Heise et al., 2018; Khanmohammadi et al., 2020; Ravarian et al., 2010). Instead, developing a biocomposite-based HA coating may improve coating strength and corrosion resistance (Nabian et al., 2011). A corrosive environment in the human body is mainly related to the existing chloride ions, which influence biological responses such as corrosion in the blood plasma environment. This state can also affect the biocompatibility of the implant material, which is made of stainless steel and has a high corrosion resistance (Al-Rashidy et al., 2015; Bagherifard et al., 2015). By removing metallic ions and electrons from metallic implants, a passive oxide layer may form to protect the surface material from corrosion. (Manam et al. 2017). Additionally, Sources of corrosive ions include water, dissolved oxygen, chloride, and other electrolytes bicarbonate, traces of potassium, calcium, magnesium, phosphate, sulphate, amino acids, proteins, and plasma. Toxic nickel, for example, could be released through chloride ion corrosion of stainless steel, causing allergic reactions such as skin expansion, edema, and, eventually,

tissue around the implant (Bagherifard et al. 2016). Metal ions can affect histology and induce tumors in detoxication organs (liver, kidney, and spleen) (Manam et al. 2017).

Surface treatments of biomedical items, in general, have potentially alleviated corrosion problems rather than increasing biocompatibility. This method may employ coating materials that provide good surface osteoconductivity and corrosion protection (Kravanja and Fingar, 2022). Dip coating, thermal spraying (Cheang and Khor, 1995), physical vapor deposition (Geyao et al., 2020), laser cladding (Comesaa et al., 2010), and electrophoretic deposition (EPD) (Thanh et al., 2015) are all methods that are available for coating metallic implants with HA. The EPD approach, for example, can be used for the surface coating of bioceramics, polymers, and composites on metallic implants for biomedical applications (Besra and Liu, 2007). Furthermore, the EPD process relates to an electrochemical mechanism in which charged ions migrate to the opposite charge electrode surface under the influence of an electric field (Pani et al., 2022). This approach has a wide range of biomedical applications because of its versatility, simplicity, cost-effectiveness, and applicability to complex shapes (Besra and Liu, 2007; Ma et al., 2003; Paniet al., 2022; Thanh et al., 2015).

Recently the EPD technology has demonstrated a promising approach for manufacturing bulk HA scaffolds for biological applications (Kravanja and Fingar, 2022). Many biocompatible coating materials exist, including hydroxyapatite [HA, $Ca_{10}(PO_4)_6(OH)_2$], calcium silicate (CS, $CaSiO_3$), α-tricalcium phosphate (α-$Ca_3(PO_4)_2$ or β-TCP), tetra calcium phosphate [$Ca_4(PO_4)_2O$ or TTCP], and calcium oxide (CaO). However, researchers have found it difficult to deposit a thick HA deposit on metallic objects with sufficient bioactivity. Accordingly, only a limited study on using the EPD method for coating hydroxyapatite of metallic implants was available in the literature. Furthermore, several in vivo and clinical investigations omitted chemical and structural characterization of the coatings, making comparisons of experimental results between research difficult.

In the current study, stainless steel alloy (SS316L) plates were coated with hydroxyapatite (HA) powder precursor suspended in ethanol with nitric acid by direct current electroplating (DC-EPD). During the EPD procedure, temperatures in the 30-50°C range and stirring speeds (90, 120, and 150 rpm) were varied. The surface of the coated plates was examined for phase and porosity distribution using X-ray diffraction (XRD) and optical microscopy. Instead, surface response methodology (SRM) can estimate coating mass output by optimizing EPD parameters (temperatures and stirring speeds). It was possible to gain insight into the formation of thick HA deposits with homogeneous porosities in this study.

2. MATERIALS AND METHOD

2.1 Colloidal solutions and substrates

Stainless steel (AISI SS316L) substrate plates with sizes 25 x 10 x 1 mm were the working and counter electrodes selected.Each substrate was thoroughly cleaned by ultrasonically bathing it in high-purity water (Fischer Bioblock Scientific). To make colloidal solution with a concentration of 2 g/L, 0.5 g of hydroxyapatite powder precursors (Merck, Analytical grade > 90 %) was blended with 250 mL of ethanol (C_2H_5OH)(998.6%). Subsequently, a produced ethanol colloidal solution was mixed with HNO_3 (3mM) to reach a pH value of 3. After cleaning, the plates were in the colloidal solution, which was agitated for 60 minutes at 200 rpm with a magnetic stirrer before the APD process.

2.2 Electrophoretic Deposition Experiments

The EPD experiment was to investigate the effects of temperature and stirring speed on coating mass yield. The experimental parameters are a constant electric field of 30 V and a 5-minute operating duration at different temperatures (30, 40, and 50°C) and stirring rates of 90, 120, and 150 rpm in the colloidal solution pH 3. The EPD cell consists of a graphite plate cathode and the anodic electrode of stainless steel of SS316L with a cathode-anode distance of 20 mm and a deposition area of 2.5 cm2. The coated samples were air-dried for 24 h at the

end of the process. Furthermore, a deposited mass (m) resulting from deposition at low voltages and short deposition durations is as follows according to Hamaker's law (Eq.1)(Hamaker, 1940):

$$m = \mu \times Cs \times A \times E \times t \qquad (1)$$

Where deposited mass m (in gram), electrophoretic mobility μ (in $cm^2/s*V$), solids concentration Cs (in g/cm^3), coated surface area A (cm^2), electric field strength E (V/cm), and time t (seconds) are all given. A particle's electrophoretic mobility characterizes its velocity in the presence of an applied field as Eq. (2).

$$\mu = \frac{V}{E} \qquad (2)$$

The efficiency of the EPD method can be computed to theoretical values using these equations. In addition, the SRM model used two quadratic polynomial equations (Eq. 3) to relate the reaction of yield mass coatings versus EPD parameters utilizing the design expert application. Two responses were to solve the polynomial equations, allowing researchers to investigate the correlations between responses and deposition parameters.

$$y = \beta_0 + \sum_{i=1}^{k} \beta_i x_i + \sum_{i=1}^{k} \beta_{ii} x_i^2 + \sum \sum_{i<j}^{\infty} \beta_{ij} x_i x_j + \varepsilon \qquad (3)$$

Where Y stands for the dependent variable, β_0 stands for the constant coefficient, Xi stands for the ith independent variable, and Xj stands for the jth independent variable. The independent variables X_1 and X_2 are electrode distance and time, respectively. The linear effect by bi relates to the squared effect by bii and the interaction effect of the variables Xi and Xj by bij.

2.3 Surface characterisation

The XRD data from the coated surface was acquired using an X-ray diffractometer (XRD 6000, Shimashu, Japan) with Cu-Kα (λ=0.15406 nm) radiation and compared to the XRD of

the substrate SS316L plates. Furthermore, for qualitative characterization, a QualX search-match program verified the phases created by the coating process (Altomare et al., 2008). The surface morphology and cross-sections of the coated samples were analysed using an optical microscope (Olympus BX53M). In this case, the coating mass relates to the mass difference between the uncoated and coated sections.

3. Results and Discussion

3.1. EPD coatings

Electrophoretic depositions with hydroxyapatite reagents in acidic pH suspensions with nitric acid resulted in the white coating powder on the surface. The coating mass was estimated using Haymaker's equation (Eq. 1) and electrophoretic mobility data (μ) from the reported data (Hanaoret al., 2011). This equation did not account for the coating's insulating effects on the electrical field strength, which was supposed to be 5V/cm, as well as the decrease in the solids loading of the suspension as deposition occurred. Table 1 presents the results of electrophoretic deposition, including a comparison of the estimated deposit mass based on Eq. (1) with the measured deposit mass acquired from acidic solution anodic electrophoretic depositions employing pH adjustment agents. The use of nitric acids increased deposition rates when agitated at low temperatures and rising speeds. Despite higher-than-expected rates, nitric acids had considerable control over deposition rates as temperatures and stirring speeds increased. Although increasing the deposition rate required reduced deposition current with increased temperature and stirring rates, the available electrical current of suspension fluctuated and decreased over time(Figure 1).

Table-1. The resulting deposited mass on SS 316L plate

Run	Parameter (Temp. & str. speed)	Uncoated mass (mg)	Coated mass (mg)	Deposited mass (mg)	Calculated mass (mg)
1	30^{O}C & 90 rpm	1.9280	1.9318	0.0038	0.00383
2	30 ^{O}C &120 rpm	1.9271	1.9289	0.0018	0.00383
3	30 ^{O}C &150 rpm	1.9274	1.9314	0.0040	0.00383
4	40 ^{O}C &90 rpm	1.9275	1.9296	0.0021	0.00383
5	40 ^{O}C &120 rpm	1.9252	1.9283	0.0031	0.00383
6	40 ^{O}C &150 rpm	1.9262	1.9295	0.0033	0.00383
7	50 ^{O}C &90 rpm	1.9285	1.9300	0.0015	0.00383
8	50 ^{O}C &120 rpm	1.9223	1.9271	0.0048	0.00383
9	50 ^{O}C &150 rpm	1.9255	1.9353	0.0098	0.00383

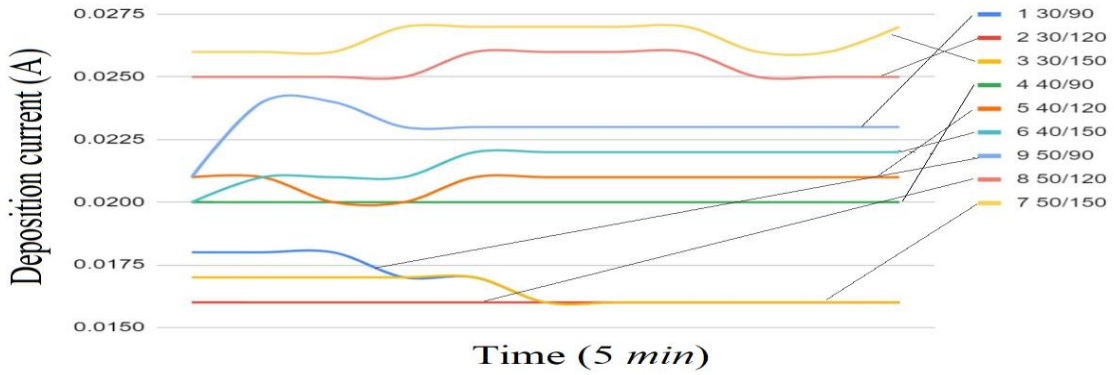

Figure-1. The deposition current (in Ampere) needed to produce the deposited mass during the 5-minute operating duration.

Furthermore, SRM (surface response methodology) generated the optimized EPD parameters for the required coating deposition yield. According to Eq. 3, Figure 2a depicts the 2D-response surface plots for the interaction influence of temperature (X_1) and stirring speed (X_2) on deposition mass yield (Y). According to the contour plots, a higher temperature and a faster stirring speed result in a coating with a high yield mass. The optimal settings for the high yield of coating mass (> 8 mg) under the indicated constraints related to temperatures of 45-50 °C, stirring speeds of 140-150 rpm, a 5-minute operation duration, and a voltage of 30 V.

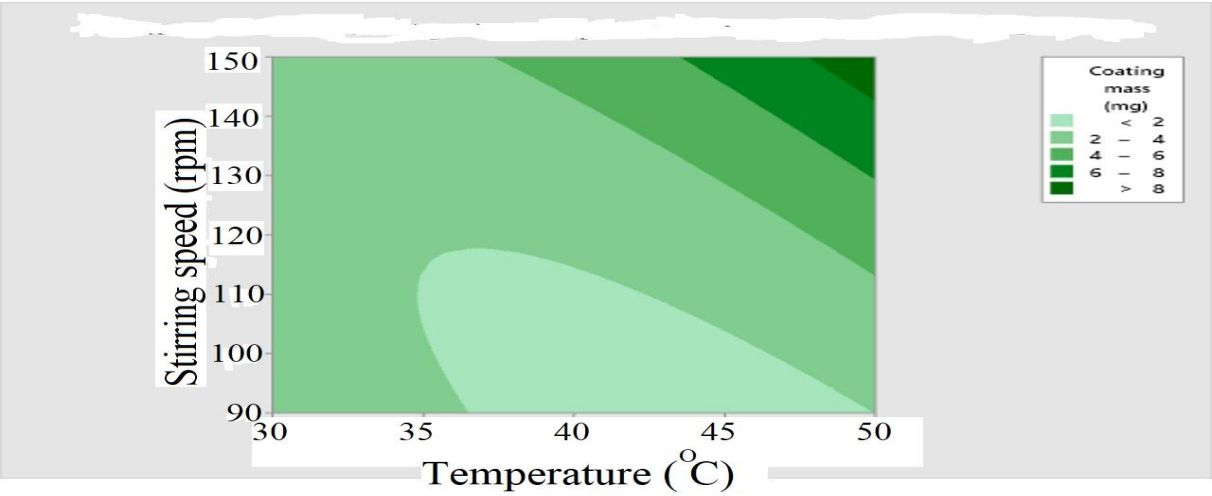

Figure-2. Temperature and stirring speed influences on deposition mass during a 5-minute operation.

Optical microscopy captured images of the deposited SS316L stainless steel. Pinholes on coating surfaces caused by trapped gas bubbles in the coating are in these photos. These gas bubbles are most likely the product of water electrolysis, a previously documented parasitic mechanism. Surface coatings with nitric acid-altered pH values had numerous little pinhole sizes ranging from 5 to 10 µm (Fig. 3). The acidic solution coatings have uneven and poor coverage, resulting in a low deposited mass per unit area measurement.

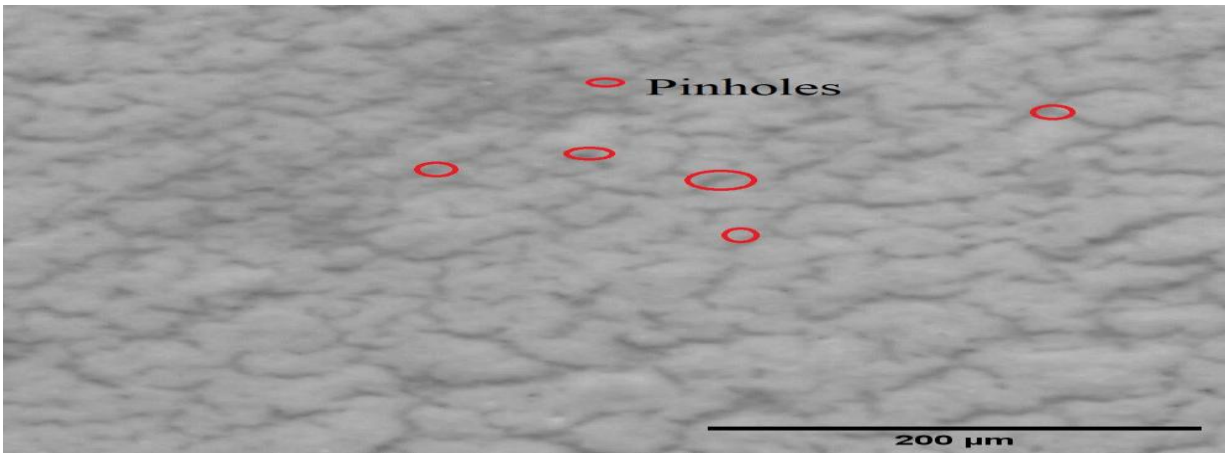

Figure-3.EPD coatings typically produced at 50 ^{O}C and 150 rpm-stirring speed from acidic solutions including nitric acids with a pH of 3

3.2 XRD Analysis

Initially, as received x-ray diffraction (XRD) data were matched with the Crystallography Open Database (COD) database for phase identification using the software program QualX [33]. A search-matching approach was followed by detecting the background, searching for matching line peaks, and showing the results in an X-ray diffractogram. -TCP phases were matched throughout the search-match methods using the reference data of COD card#7217892 (Figure 3). Thorough XRD Rietveld crystal structure analyses supported the -TCP crystal structure, which closely matched those found in the literature. The convincing Bragg peaks of the crystalline α-TCP phases between 25 and 40^{O} 2θ appear to have blended with a noticeable hump (background). The 2θ-range phase development of amorphous-calcium phosphates (ACP) may relate to a short-range order structure in this circumstance. This process may also result in changes in phase composition (amorphous and crystalline phases) rather than pure phase transitions. It is also necessary to post-heat the coating at temperatures exceeding 600°C to improve its crystalline layer.

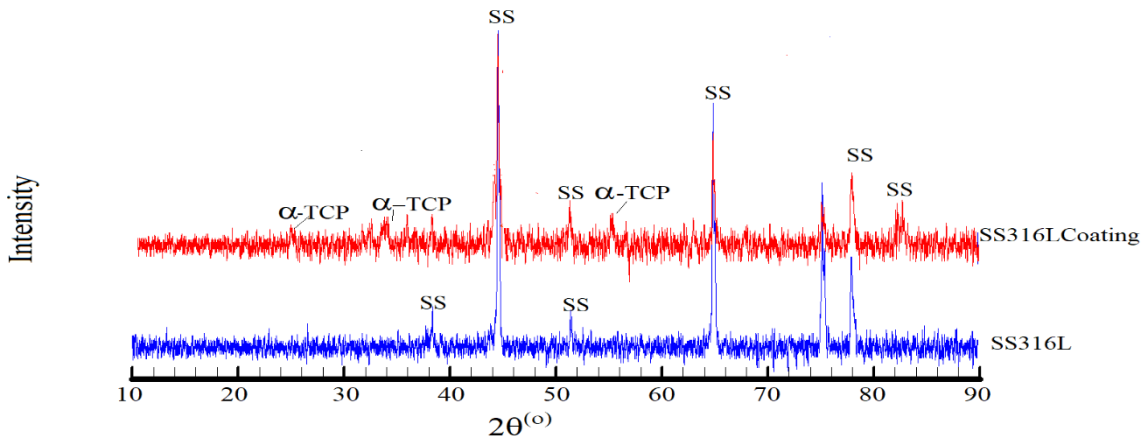

Figure-3. X-ray diffractogram of SS316 substrate with HA powder precursor coating

3.3 The study's important discovery

The surface of stainless steel was coated with hydroxyapatite powder utilizing the EPD process for orthopedic implants to enhance bioactivity through osseointegration (direct

bonding with bone). In this study, the EPD coating method resulted in metallic implant surfaces with bone-like α-TCP (α-tetra calcium orthophosphate) deposited, boosting bioactivity and enhancing osseointegration. The current work proved the potential of EPD techniques for coating stainless steel (SS316L), a material widely used in orthopedic implants. This SS316L alloy coated with bone-like α-TCP may increase its bioactivity in vitro and in vivo. This test coating resulted in a thinner calcium orthophosphate layer with high particle homogeneity and porosity (greater than 90%).

Principally, α-TCP is a ceramic widely used in orthopedic and dental cement made by solid-state reactions occurring at low temperatures making temperature and stirring speed control critical in the EPD method to avoid secondary phase formation such as α-TCP. TCP is available in two polymorphs: α-TCP and β-TCP. The β-TCP phase is more stable and biocompatible than the α-TCP phase. New bone may develop in the previously occupied location as the α-TCP resorbs. In this scenario, polymorph β-TCP is transformed into α-TCP by heating the non-crystalline powder at low temperatures or by thermal crystallization above the transformation point (Dorozhkin et al., 2014). In particular, unlike hydroxyapatite, α-TCP material has strong osteoconductivity but poor osteoinductivity. As a result, α-TCP is appropriate for diseases requiring implant material resorption, followed by host bone rebuilding (Klein et al., 1999).

The current research on the synthesis of α-TCP involves the thermal transformation of a powder precursor of ACP (amorphous calcium phosphate) or CDHA (calcium-deficient hydroxyapatite) with a Ca/P molar ratio of 1.5 (Arcos and Vallet-Reg, 2020; Carrodeguas and De Aza, 2011; Eliaz and Sridhar, 2008). The experimental EPD coating in this work demonstrated that hydroxyapatite decomposes to α-TCP after about 5 minutes in an acidic solution at temperatures less than 50 ^{O}C, followed by water dehydration (Eq. 4).

$$Ca_9(HPO_4)\,(PO_4)_5(OH)\,(s) \rightarrow 3\alpha\text{-}Ca_3(PO_4)_2\,(s) + H_2O\,(g) \qquad (4)$$

As a result, the α-TCP coating on stainless steel should have good osteoconduction properties while emphasizing bioactive properties. α-TCP formation is most likely the best coating for assessing the bioactivity of orthopedic materials. Improving osteoconduction needs more research on β-TCP specimens implanted on cancellous bone in rabbit tibia. However, research may be performed on the compositional properties of various powder precursors and efforts to increase coating kinetics and strength.

4. CONCLUSION

The current work showed that coating SS316L- substrates with α-TCP results in a thin covering. The surface coating included uniformly distributed porosity, enabling quicker tissue growth and osseointegration. The biomedical standard requires a coated surface roughness with high adhesion strength. The α-TCP phases formed on the surface coating with high amorphous phases may be great resorbability. However, the procedure requires a solvent media selection to provide suspension stability and good electrophoretic mobility. More research is needed, however, to obtain insight into the mechanisms through appropriate modeling of the process and charge generation in non-aqueous suspensions for suspension stability and deposition control strength.

Acknowledgments

The authors would like to thank Diponegoro University in Indonesia for funding the PMDSU (*Pendidikan Magister menujuDoktoruntukSarjanaUnggul*) scholarship.

Disclosure statement

The author reported no potential conflict of interest

Funding

Diponegoro University, Indonesia, provided financial support for this work under PMDSU Grant Number: 14-03/UN7.P4.3/PP/2021.

REFERENCES

Al-Rashidy,Z.M.,Farag,M.M., Abdel Ghany,N.A., Ibrahim,A.M., Abdel-Fattah, W.I (2017) Aqueous electrophoretic deposition and corrosion protection of borate glass coatings on 316 L stainless steel for hard tissue fixation. *Surfaces and Interfaces* 7, 125-133. https://doi.org/10.1016/j.surfin.2017.03.010

Altomare, A., Cuocci, C Giacovazzo, C., Moliternia, A., Rizzia, R. (2008) QUALX: a computer program for qualitative analysis using powder diffraction data.*Journal of Applied Crystallography* 41, 815-817. https://doi.org/10.1107/S0021889808016956

Arcos D., Vallet-Regí, M. (2020) Substituted hydroxyapatite coatings of bone implants. *Journal of Materials Chemistry* B8, 1781–1800. https://doi.org/10.1039/C9TB02710F

Bagherifard,S., Hickey,D. J., de Luca, A. C., Malheiro,V. N.,Markaki, A. E., Guagliano, M., Webster,T. J. (2015) The influence of nanostructured features on bacterial adhesion and bone cell functions on severely shot peened 316L stainless steel. *Biomaterials* 73, 185-197. https://doi.org/10.1016/j.biomaterials.2015.09.019

Bagherifard,S. Slawik,S. Fernández-Pariente,I., Pauly,C.,Mücklich,F., Guagliano, M. (2016) Nanoscale surface modification of AISI 316L stainless steel by severe shot peening, *Materials & Design* 102, 68-77. https://doi.org/10.1016/j.matdes.2016.03.162

Besra,L., Liu, M. (2007) A review on fundamentals and applications of electrophoretic deposition (EPD). *Progress in Materials Science* 52(1) 1-61 https://doi.org/10.1016/j.pmatsci.2006.07.001

Carrodeguas, R.G, De Aza S. (2011) Review: α-Tricalcium phosphate: synthesis, properties and biomedical applications. *ActaBiomaterialia*7, 3536–3546.https://doi.org/10.1016/j.actbio.2011.06.019

Cheang,P., Khor, K.A. (1995)Thermal spraying of hydroxyapatite (HA) coatings: Effects of powder feedstock.*Journal of Materials Processing Technology* 48(1–4), 429-436.https://doi.org/10.1016/0924-0136(94)01679-U

Comesaña,R., Quintero,F.,Lusquiños,F.,Pascual,M.J.,Boutinguiza,M., Durán,A., Pou,J. (2010) Laser cladding of bioactive glass coatings. *ActaBiomaterialia* 6(3), 953-961. https://doi.org/10.1016/j.actbio.2009.08.010

Dorozhkin, S. V. (2014) Calcium orthophosphate coatings on magnesium and its biodegradable alloys. *Acta Biomaterialia*10, 2919–2934. http://dx.doi.org/10.1016/j.actbio.2014.02.026.

Eliaz, N., Sridhar, T.M.(2008) Electrocrystallization of hydroxyapatite and Its dependence on solution conditions. *Crystal Growth & Design* 8, 3965–3977. https://doi.org/10.1021/cg800016h.

Ferrari B, Moreno R. (2010) EPD kinetics: a review. *Journal of the European Ceramic Society***30**(5):1069–78.https://doi.org/10.1016/j.jeurceramsoc.2009.08.022

Gao, F., Xu, C., Hu,H.,Wang,Q., Gao,Y.,Chen,H., Guo,Q., Chen, D., Eder, D.(2015) Biomimetic synthesis and characterization of hydroxyapatite/graphene oxide hybrid coating on Mg alloy with enhanced corrosion resistance. *Materials Letters*, 138, 25-28D. https://doi.org/10.1016/j.matlet.2014.09.088

Gebhardt,F., Seuss,S., Turhan,M.C., Hornberger,H., Virtanen,S.,Boccaccini,A.R. (2012) Characterization of electrophoretic chitosan coatings on stainless steel. Materials Letters, 66 (1), 302-304. https://doi.org/10.1016/j.matlet.2011.08.088

Geyao,L., Yang,D.,Wanglin,C.,Chengyong, W. (2020) Development and application of physical vapor deposited coatings for medical devices: A review. Procedia CIRP 89, 250-262. https://doi.org/10.1016/j.procir.2020.05.149

Hamaker H. (1940) Formation of a deposit by electrophoresis. *Transactions of the Faraday Society* **35**:279–87.https://doi.org/10.1039/TF9403500180

Hanaor,D.,Michelazzi,M., Veronesi,P., Leonelli,C., Romagnoli,M., Sorrell,C. (2011)Anodic aqueous electrophoretic deposition of titanium dioxide using carboxylic acids as dispersing agents.*Journal of the European Ceramic Society* 31, 1041–1047.https://doi.org/10.1016/j.jeurceramsoc.2010.12.017

Heise,S., Wirth,T.,Höhlinger,M., Hernández,Y. T., Ortiz,J. A. R., Wagener,V., Virtanen,S.,Boccaccini, A. R. (2018) Electrophoretic deposition of chitosan/bioactive glass/silica coatings on stainless steel and WE43 Mg alloy substrates.*Surface and Coatings Technology* 344, 553-563. https://doi.org/10.1016/j.surfcoat.2018.03.050.

Jeon, T., Na, Y.E., Jang, D., Kim, I.W. (2020) Stabilized amorphous calcium carbonate as a precursor of microcoating on calcite. *Materials (Basel).*13, 1–11.http://dx.doi.org/10.3390/ma13173762

Khanmohammadi,S.,Ojaghi-Ilkhchi,M., Farrokhi-Rad,M. (2020) Evaluation of bioglass and hydroxyapatite based nanocomposite coatings obtained by electrophoretic deposition. *Ceramics International* 46(16), Part A, 26069-26077.https://doi.org/10.1016/j.ceramint.2020.07.100

Kravanja,K. A.,Finšgar,M. (2022)A review of techniques for the application of bioactive coatings on metal-based implants to achieve controlled release of active ingredients,*Materials & Design*, 217, 110653.https://doi.org/10.1016/j.matdes.2022.110653.

Ma,J., Wang,C., Peng,K.W. (2003)Electrophoretic deposition of porous hydroxyapatite scaffold. *Biomaterials* 24, 3505-3510.https://doi.org/10.1016/S0142-9612(03)00203-5.

Manam,N.S., Harun,W.S.W., Shri,D.N.A., Ghani,S.A.C., Kurniawan,T., Ismail, M.H., Ibrahim,M.H.I. (2017)Study of corrosion in biocompatible metals for implants: a review.*Journal of Alloys and Compounds*, 701,698-715.https://doi.org/10.1016/j.jallcom.2017.01.196

Mathew, M., Schroeder, L.W., Dickens, B., Brown, W.E (1977) The crystal structure of α-Ca3(PO4)2. *Acta Crystallographica* Section B. 33, 1325-1333. https://doi.org/10.1107/S0567740877006037.

Nabian,N., Jahanshahi,M.,Rabiee,S. M. (2011) Synthesis of nano-bioactive glass–ceramic powders and its in vitro bioactivity study in bovine serum albumin protein, *Journal of Molecular Structure*, 998(1–3),37-41. https://doi.org/10.1016/j.molstruc.2011.05.002

Overgaard, S. (2009) Degradation of calcium phosphate coatings and bone substitutes Cell. Response to Biomater. Woodhead Publishing Limited; 2009. http://dx.doi.org/10.1533/9781845695477.3.560.

Pani,R., Behera,R. R., Roy,S. (2022)Electrophoretic deposition of hydroxyapatite Coating: A state of art, *Materials Today: Proceedings*,62(6),4086-4093,https://doi.org/10.1016/j.matpr.2022.04.632.

Ravarian,R.,Moztarzadeh,F.,SolatiHashjin,M.,Rabiee,S.M.,Khoshakhlagh,P.,Tahriri, M (2010) Synthesis, characterization and bioactivity investigation of bioglass/hydroxyapatite composite. *Ceramics International* 36(1), 291-297. https://doi.org/10.1016/j.ceramint.2009.09.016.

Samani,F. Y.,Rabiee,S. M.,Jamaati,R.,Bagherifard,S. (2023) Effect of shot peening on electrophoretic deposition of bioactive glass coating on AISI 316L stainless steel.*Ceramics International*, 49(11), Part A, 17468-17478. https://doi.org/10.1016/j.ceramint.2023.02.114

Thanh, D. T. M.,Nam,P. T., Phuong,N. T., Que,L. X., Anh,N. V., Hoang, T., Lam,T. D. (2013)Controlling the electrodeposition, morphology and structure of hydroxyapatite coating on 316L stainless steel.*Materials Science and Engineering*: C 33(4), 2037-2045, https://doi.org/10.1016/j.msec.2013.01.018

Vladescu,A.,Padmanabhan,S.C., Ak Azem,F.,Braic,M.,Titorencu,I., Birlik,I., Morris,M.A.,Braic,V. (2016)Mechanical properties and biocompatibility of the sputtered Ti doped hydroxyapatite.J. Mech. Behav. Biomed. Mater.Journal of the Mechanical Behavior of Biomedical Materials 63, 314-325.https://doi.org/10.1016/j.jmbbm.2016.06.025